

Study on Continuous Flow Nitration of Naphthalene

Feng Xu, Zhiqian Chen,* Lei Ni, Gang Fu, Jian Liu, and Juncheng Jiang*



Cite This: *Org. Process Res. Dev.* 2023, 27, 2134–2145



Read Online

ACCESS |

Metrics & More

Article Recommendations

Supporting Information

ABSTRACT: In this work, the continuous flow nitration of naphthalene to 1-nitronaphthalene was systematically studied from the microreactor to mesoscale flow reactor and the safety issues during the reaction process were investigated. The effect of the molar ratio of nitric acid to naphthalene, residence time, reaction temperature, and sulfuric acid strength on the reaction process was comprehensively investigated in the microreactor. Under optimal conditions, the reaction yield could reach 94.96%. Due to the rapid exothermic characteristics of nitration, a quick heat transfer assessment was proposed to obtain the temperature profile during optimal conditions. It was found that the maximum overtemperature during the reaction was only 3.78 °C, which was consistent with the high yield under the optimal conditions. Then a scale-up of the microreactor to production was realized by a dimension-enlarging strategy. In the mesoscale flow reactor, the influence of volumetric flow rates was investigated. The annual output of the flow reactor could reach 2643 kg·a⁻¹ while the highest overtemperature inside the reactor channel well exceeded 17.1 °C. In addition, a conventional semibatch experiment was carried out in the batch calorimeter RC1e to explore the reaction's exothermic characteristics. Finally, the performances of the two reactors were compared, showing that the continuous flow reactor had more advantages than the batch reactor in economic benefit and inherent safety.

KEYWORDS: nitration, 1-nitronaphthalene, flow chemistry, scale up, heat transfer assessment

1. INTRODUCTION

Mixed acid nitration of aromatic compounds is widely used to produce a series of essential intermediates such as drugs, dyes, explosives, and pesticides.^{1,2} However, most nitration processes are fast and highly exothermic, with the heat of the reaction ranging from -73 to -253 kJ·mol⁻¹.³ Many of the products have thermal decomposition characteristics, which is quite dangerous.^{4,5} As one of the important intermediates, 1-nitronaphthalene is currently produced through the nitration of naphthalene using a mixed acid in the batch reactor. Considering the safety issues during the reaction process, the reaction is usually performed by slowly dropping the mixed acid into the organic substrate, which makes the production less efficient. Therefore, it is necessary to improve the production efficiency and reaction safety through process enhancement.

Flow chemistry, as a process enhancement technology, has attracted increasing attention in the chemical and pharmaceutical industries in recent years.⁶ The continuous flow microreactor with a smaller characteristic size and larger specific surface area is considered an excellent tool for performing such fast and exothermic reactions due to enhanced mixing and heat transfer capacity.^{7–10} A smaller liquid holdup is conducive to the inherent safety which can operate more efficiently and safely under much harsher conditions.^{11,12} The residence time in the microreactor can be precisely controlled, which provides a basis for the kinetic study of those rapid reactions. In recent years, many researchers have successfully realized nitration process enhancement, combining various needs of aromatic nitration and the advantage of microreactors.¹³ Burns et al.¹⁴ investigated the continuous flow nitration of toluene and

benzene, showing that slug flow within the microreactor can provide enough effective interfacial area for fast liquid–liquid heterogeneous reaction. Su et al.¹⁵ performed nitration of *o*-nitrotoluene in the packed microreactor. Due to the outstanding dispersion and mass transfer capacity of the packed microreactor, the conversion of nitrotoluene reached up to 94% even when the reaction was less than 3 s. Yu et al.¹⁶ carried out the rapid selective nitration of 1-methyl-4-methylsulfonyl benzene in a microreactor, and the reaction yield reached 98% in a very short time. Wen et al.¹⁷ performed a continuous flow nitration of trifluoromethoxybenzene in the microchannel reactor. The highest conversion could reach 99.6%, and the main product selectivity could reach 98.13% under the optimal conditions. Li et al.¹⁸ conducted experimental and kinetic studies of the nitration of 2-ethyl hexanol based on the outstanding mass transfer characteristics of the microreactor and the pseudohomogeneous assumption. Under the best reaction conditions, the yield could reach 99% within 10 s. Chen et al.¹⁹ conducted research on the synthesis of 5-fluoro-2-nitrotrifluoro-toluene in a microreactor, and the results suggested that when the molar ratio of HNO₃/H₂SO₄/C₇H₄F₄ was 3.77/0.82/1, the reaction yield could reach 96.4%. Zhao et al.²⁰ studied the reaction of benzene and hydrogen peroxide catalyzed by solid metavanadate to produce phenol in the microreactor, and under the optimal conditions, the yield

Received: August 17, 2023

Published: October 16, 2023



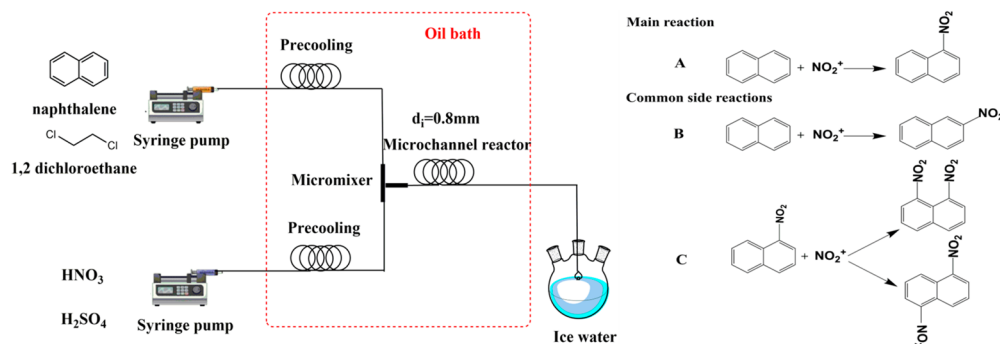


Figure 1. (a) Schematic of the microreactor reaction system and (b) scheme for the nitration of naphthalene with mixed acid.

can reach 15%, and the selectivity can reach 94%. In the same year, Hussain et al.²¹ utilized the outstanding mass and heat transfer capacity of the flow reactor and realized scale-up of the synthesis of selective herbicide pendimethalin at 50 kg/day in the pilot-scale plant. Cui et al.²² measured the kinetics of chlorobenzene nitration based on the precise control of the reaction time in the microreactor, and the results showed that for chlorobenzene nitration, the apparent reaction rate constant was on the order of $10^{-4}\text{ L}\cdot\text{mol}^{-1}\cdot\text{s}^{-1}$, and the reaction activation energy was around $25\text{ kJ}\cdot\text{mol}^{-1}$. Many researchers have conducted reaction enhancement or kinetic studies of various nitration in the microreactor, and some of them realized process scale-up by a numbering up or sizing up approach. However, few of them combined the overtemperature during the reaction with the process safety in the continuous flow mode and compared the flow mode with the batch mode by experiments.

In this study, the continuous flow nitration of naphthalene to 1-nitronaphthalene was systematically studied, combining process optimization with process safety. First, the influence of key operating parameters including molar ratio, reaction temperature, sulfuric acid strength, and residence time was systematically studied in the microreactor. And by studying the apparent reaction rate constant under the optimal conditions, the energy conservation equation was coupled with the mass conservation equation to quickly estimate the temperature profile of the reaction along the microchannel under the optimal conditions. Then the process was scaled up by the dimension-enlarging methodology while considering process safety, and the temperature profile in the mesoscale flow reactor under optimal conditions was studied with the real-time temperature monitoring system. Finally, a comparison between the semibatch mode and continuous flow mode was carried out to show the superiority of the continuous flow reactor in production efficiency and inherent safety.

2. EXPERIMENTAL SECTION

2.1. Reagents. Fuming nitric acid (>98%, Sinopharm Chemical Reagent Co., Ltd.), sulfuric acid (>98%, Sinopharm Chemical Reagent Co., Ltd.), naphthalene (CP, Sinopharm Chemical Reagent Co., Ltd.), 1,2-dichloroethane ($\geq 98.5\%$, Sinopharm Chemical Reagent Co., Ltd.), 1-nitronaphthalene (>95%, Aladdin Reagent Co., Ltd.), 2-nitronaphthalene ($\geq 98\%$, Aladdin Reagent Co., Ltd.), dinitronaphthalene ($\geq 97\%$, Aladdin Reagent Co., Ltd.), acetonitrile (HPLC, Sinopharm Chemical Reagent Co., Ltd.). H₂SO₄ (less than 98%) was prepared by diluting H₂SO₄ with deionized water. All reagents were used without further purification.

2.2. Experimental Setup. The experimental setup is demonstrated in Figure 1a. The organic phase was formed by dissolving 0.1 mol of naphthalene in 0.4 mol of dichloroethane. And the aqueous phase was a mixture of water, sulfuric acid, and nitric acid. The organic phase and the aqueous phase were injected through two syringe pumps, respectively. First, the two phases were reacted in a T-shaped mixer made of stainless steel. The main reaction and common side reactions are shown in Figure 1b. Then the mixed liquid reacted in a Teflon microchannel with an inner diameter $d_i = 0.8\text{ mm}$ and an outer diameter $d_o = 1.6\text{ mm}$. All the channels were immersed in an oil bath to obtain a uniform reaction temperature. The total volumetric flow rate of the mixed fluid was maintained at $3\text{ mL}\cdot\text{min}^{-1}$, and the residence time was regulated by changing the channel length. The molar ratio was controlled by the volumetric flow rate ratio of the two phases. The reaction product from the outlet of the reactor channel was immediately quenched with an ice–water bath. Then the reaction product was quickly separated and washed. HPLC was used to analyze the product.

The mesoscale flow reactor platform is depicted in Figure 2.

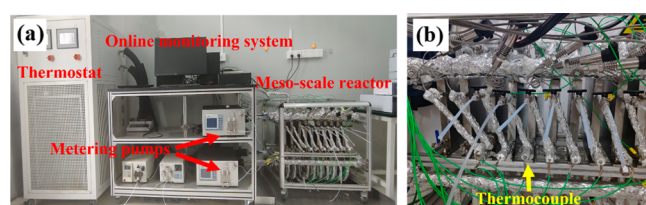


Figure 2. Images of the Hastelloy continuous flow reactor platform (a) photo of the reaction platform; (b) photo of the flow reactor whose channel outer diameter was $1/4\text{ in.}$ and wall thickness of the channel was 1 mm .

Two metering pumps (Xingda, 2PB-10005III; Tauto, TBP-1H02SF, China) were used to deliver the organic phase and aqueous phase into the mesoscale reactor. And the two phases were preheated to the setting temperature by the first two modules of the reactor, respectively. The following modules, whose liquid holdup is 32 mL, were all modules for reaction. To control the reaction temperature, a thermostat (Jiangsu Haisi Temperature Control Equipment Co., Ltd., China) with two independent systems was used. Finally, when the reaction system was stable, the reaction product at the outlet was quickly quenched in ice water for sample analysis. During the reaction process, the pressure and temperature inside different modules were measured by pressure transmitters and thermocouples.

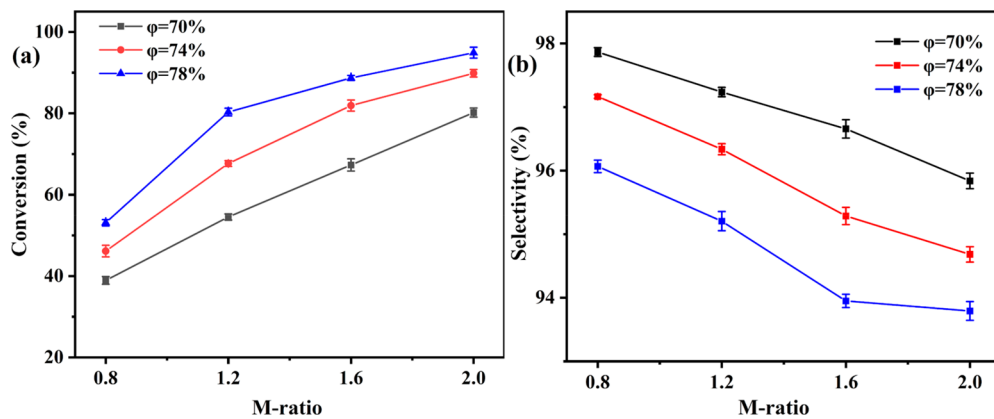


Figure 3. Effect of the molar ratio on reaction (a) conversion and (b) selectivity. When the residence time was 20 s and the reaction temperature was 35 °C.

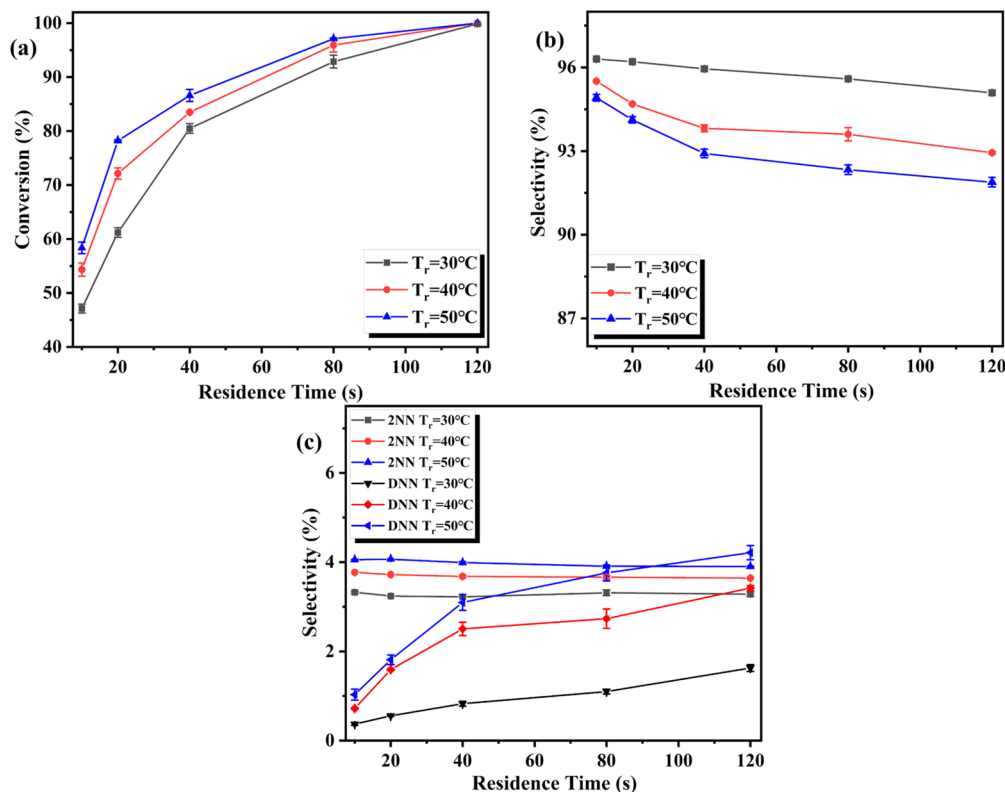


Figure 4. With the 74% sulfuric acid strength and the molar ratio of 1.2, the effects of residence time and reaction temperature on reaction (a) conversion, (b) selectivity of the main product, and (c) selectivity of byproducts.

2.3. Sample Analysis. After the collected sample was separated, the organic layer was obtained and dissolved in acetonitrile in a particular proportion. Then, a high-performance liquid chromatography device (Agilent-1260, Agilent Technologies, USA) was used to analyze samples. A Poroshell 120, EC-C18 analytical column (4.6 mm × 250 nm, particle size 4 μm) was employed to carry out the HPLC analysis. The mobile phase was composed of 70% acetonitrile and 30% water at a flow rate of 0.5 $\text{mL}\cdot\text{min}^{-1}$. The column temperature was maintained at 30 °C, and the detection wavelength of the UV detector was 254 nm. The injection volume was 5 μL .

The conversion of naphthalene (X) was obtained by the following equation:

$$X = 1 - \frac{w_{\text{Nap}} \times m_{\text{or}}}{m_{\text{Nap},0}} \quad (1)$$

Then the selectivity of 1-nitronaphthalene (S) was calculated as follows:

$$S = \frac{w_{1-\text{Nap}} \times m_{\text{or}} / M_{1-\text{Nap}}}{C \times m_{\text{Nap},0} / M_{\text{Nap}}} \quad (2)$$

where w_{Nap} and $w_{1-\text{Nap}}$ are the mass fractions of naphthalene and 1-nitronaphthalene in the organic layer, respectively. m_{or} is the mass of the organic layer, $m_{\text{Nap},0}$ is the feeding mass of naphthalene, and M_{Nap} and $M_{1-\text{Nap}}$ are the molar mass of naphthalene and 1-nitronaphthalene, respectively. The dissolved organics in the water phase were negligible.

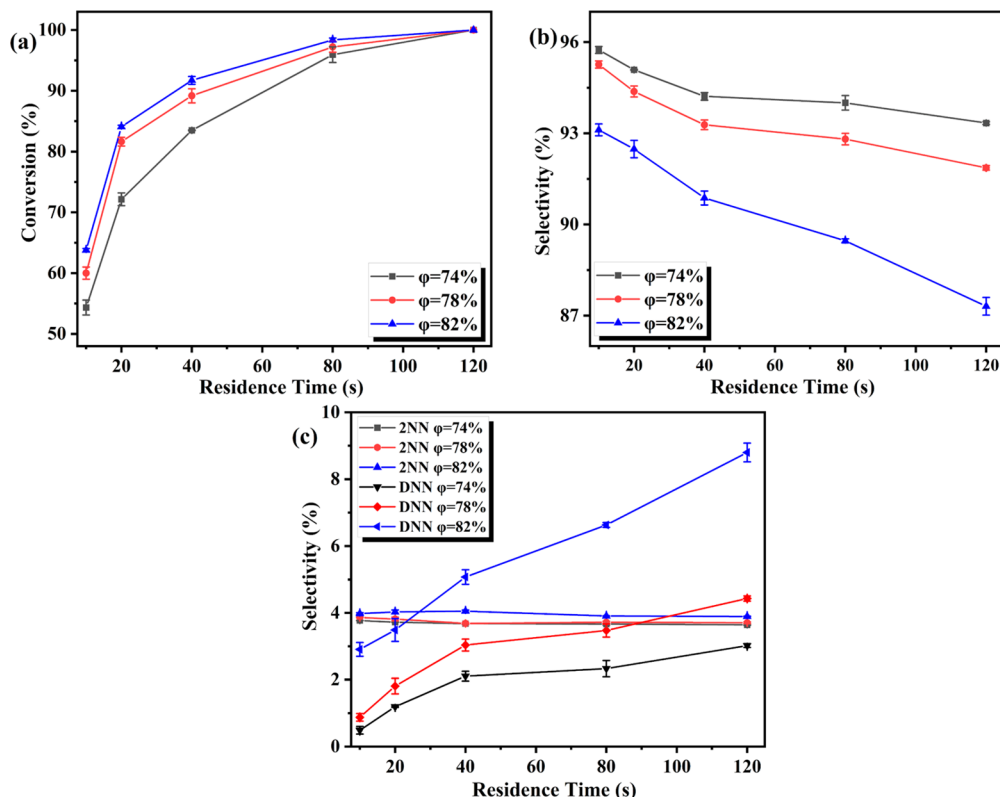


Figure 5. With $T_r = 40^\circ\text{C}$ and $M = 1.2$, the effect of sulfuric acid strength on reaction (a) conversion, (b) selectivity of the main product, and (c) selectivity of byproduct.

3. RESULTS AND DISCUSSION

3.1. Optimization of Reaction Conditions in the Microreactor. This article systematically studied the influences of the process parameters, such as the molar ratio of nitric acid to naphthalene, reaction temperature, sulfuric acid strength, and residence time, on the reaction conversion and selectivity. Each experiment was repeated three times to guarantee the reliability of the experimental results and obtain the optimum reaction conditions. The reaction temperature was controlled within 30–50 °C, the sulfuric acid strength was 74%–82%, and the residence time was set to 10–120 s.

3.1.1. Effect of Molar Ratio. To study the influence of the molar ratio, the residence time was controlled at 20 s, the temperature was set at 35 °C, and the sulfuric acid strength φ was increased from 70% to 78% to ensure the feasibility of the study. Figure 3 shows the experimental results.

According to Figure 3a, as the molar ratio increased, the conversion increased sharply. For nitration, aromatic compounds diffuse through the organic phase into the aqueous phase and nitrate with NO_2^{+} . With the molar ratio increased, the concentration of NO_2^{+} in the aqueous phase significantly increased, increasing the reaction rate. Since the mass transfer capacity of the microreactor was excellent, the reaction was still controlled by the reaction kinetics with the increase of NO_2^{+} in the aqueous phase. When enough aromatic compounds could enter the aqueous phase, the reaction conversion increased significantly under the same residence time.

It can be seen from Figure 3b that the selectivity decreased with the increase in the molar ratio. For the mononitration of naphthalene, the main side reactions consist of the dinitration and the generation of 2-nitronaphthalene. The former is a consecutive side reaction, while the latter is a parallel side

reaction. According to the research of Chen et al.,²³ although dinitration is a consecutive side reaction with higher activation energy, it will still be affected by the molar ratio of the reaction raw materials. Both the main reaction and the side reactions were prompted simultaneously by the kinetically positive effects with the increase in molar ratio. And as the molar ratio increased, the reaction rate increased. The occurrence of hot spots increased, further increasing the possibility of dinitration. In this case, the selectivity of the main product decreased.

However, the excessive use of nitric acid in the production will bring a large number of waste inorganic acid stream, which is environmentally unfriendly and hard to dispose of and recover.²⁴ And the excessive use of nitric acid is not economical. When the molar ratio increased from 1.2 to 1.6, the selectivity declined more quickly. Therefore, a molar ratio of 1.2 was selected to be the basis for the following research. When $M = 1.2$, the sulfuric acid strength increased from 70% to 74%, the conversion increased significantly, and the selectivity decreased less, so the sulfuric acid strength of 74% was selected as the initial sulfuric acid strength for subsequent research.

3.1.2. Effect of Residence Time and Reaction Temperature. When the sulfuric acid strength was 74%, with the extension of the residence time, the reaction conversion and selectivity at different setting temperatures are shown in Figure 4.

As depicted in Figure 4a, with an increase in residence time, the reaction time became more prolonged, and the reaction conversion increased rapidly. The conversion underwent an increasing trend with a decreasing slope due to the decrease in the reactant concentration. And according to the Arrhenius formula, with the increase in reaction temperature, the reaction

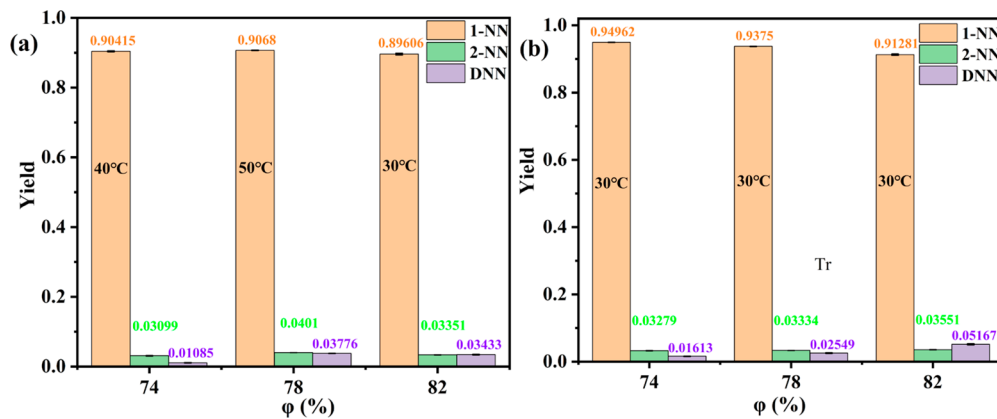


Figure 6. When the residence time was (a) 80 and (b) 120 s, the optimal reaction yield was under different sulfuric acid strengths.

rate would increase. In addition, for heterogeneous reactions, the increase in reaction temperature leads to a rise in molecular diffusion coefficient, and the mass transfer between the two phases is better.²⁵ Thus, the reaction conversion was higher under the same residence time when the reaction temperature T_r was higher.

From Figure 4b and Figure 4c, with the progress of the reaction, the 1-nitronaphthalene became dominant in the organic phase and the possibility of dinitration increased. For heterogeneous reactions, the two main factors for side reactions are poor mass transfer and local hot spots. Initially, due to the introduction of inert group nitro, the nitration activity of the naphthalene ring decreased, and it was more difficult for nitric acid to further nitrate 1-nitronaphthalene to dinitronaphthalene. However, the increase in the reaction temperature accelerated the reaction rate, and the occurrence of local hot spots increased, increasing the possibility of dinitration. Meanwhile, for the parallel side reaction, the possibility of reaching the required energy of the reaction was raised as the reaction temperature increased. Thus, the selectivity of 1-nitronaphthalene decreased with the temperature rise, which was caused by the accumulation of parallel side reaction and dinitration, especially the dinitration.

3.1.3. Effect of Sulfuric Acid Strength. Sulfuric acid not only plays the role of water absorption in the reaction but also can act as a catalyst to promote the reaction effectively.²⁶ When T_r was 40 °C, with the extension of residence time, the reaction conversion and selectivity under different sulfuric acid strengths are demonstrated in Figure 5.

As seen from Figure 5a, with the same residence time, the reaction conversion increased with the sulfuric acid strength. This is because when the sulfuric acid strength increased, the concentration of sulfuric acid in the aqueous phase increased, and the dilution effect of water generated in the reaction decreased, avoiding significant reduction of NO^{2+} due to the solvation of water. Simultaneously, the increase of sulfuric acid strength would act as a catalyst in the nitration to protonate nitric acid and generate NO^{2+} ions.²⁷

It can be seen from Figure 5b that the selectivity of 1-nitronaphthalene decreased more and more quickly with the increased sulfuric acid strength. That is because the increase in the strength of sulfuric acid would also play a catalytic role in the dinitration and parallel side reaction, making side reactions that initially require more stringent reaction conditions more likely to occur. At the same time, with the acceleration of the reaction rate, the heat transfer efficiency could no longer meet

the heat transfer demand. The occurrence of hot spots during the reaction would increase, enhancing the possibility of dinitration.

As depicted in Figure 5c, the increase in sulfuric acid strength considerably impacted the formation of dinitronaphthalene. When the sulfuric acid strength was further increased to 82%, the proportion of dinitration products increased sharply and replaced 2-nitronaphthalene as the main byproduct of the reaction.

All of the experimental information in the microreactor is shown in the Supporting Information (Figure S1). According to the influence of the above factors on the reaction conversion and selectivity during the reaction process, when T_r was 40 °C or above, or the sulfuric acid strength reached 82%, the likelihood of parallel side reactions to generate 2-nitronaphthalene and dinitration to generate dinitronaphthalene rapidly increased, leading to a significant decline in the selectivity of the main product. However, when T_r decreased or the sulfuric acid strength decreased, the reaction conversion decreased, which would bring about a decrease in yield and space-time yield. Therefore, when the residence time was 80 and 120 s, the optimal reaction yield under different sulfuric acid strengths was studied, and the results are displayed in Figure 6.

When the residence time was 80 s, with 74% and 78% sulfuric acid strength, the enhancement effect of reaction temperature on the conversion was better than the reduction on the selectivity, so the highest yields reached 40 and 50 °C, which were 90.42% and 90.68%, respectively. When the sulfuric acid strength was 82%, the influence of the temperature increase on the selectivity reduction increased, and the reaction yield was the highest at 30 °C, reaching 89.61%. When the residence time was 120 s, the reaction was completed at different temperatures, and at 30 °C, a minor side reaction occurred. So when the sulfuric acid strength was 74%, and the reaction temperature was 30 °C, the reaction yield was the highest, up to 94.96%.

3.2. Heat Transfer Assessment of the Continuous Flow Microreactor. It can be seen from the above that the reaction temperature played a critical role in the reaction yield in the flow reactor. In addition, it is widely recognized that the reaction temperature is closely associated with the reaction safety. The nitration of naphthalene is very fast with large molar reaction heat. The molar reaction heat of the nitration of naphthalene was obtained through the semibatch reaction experiment, which was about 129 kJ·mol⁻¹. So it is vital to

obtain the temperature variation during the reaction process. However, for a microreactor with an inner diameter of 0.8 mm, obtaining the temperature profile by a thermocouple is very difficult. Therefore, by coupling the heat balance equation for the nitration of naphthalene with the reaction kinetic equation, the reaction conversion and temperature profile along the channel can be roughly estimated.^{28,29}

First, the thermal balance equation is given by eq 3:

$$\rho c_p \frac{Q}{S_r} \frac{dT}{dZ} = \frac{Q}{S_r} C_0 (-\Delta H_r) \frac{dX}{dZ} - \frac{4U}{d_i} (T - T_c) \quad (3)$$

where ρ is the average mass density of the organic and aqueous phases ($1.359 \text{ g}\cdot\text{cm}^{-3}$), c_p is the average specific heat capacity ($1.45 \text{ J}\cdot\text{g}^{-1}\cdot\text{K}^{-1}$), and Q is the average volumetric flow rate ($3 \text{ mL}\cdot\text{min}^{-1}$). ΔH_r is the molar reaction heat ($-129 \text{ kJ}\cdot\text{mol}^{-1}$). Z is the channel length. S_r refers to the cross-sectional area of the microreactor channel (0.005026 cm^2), T refers to the temperature of the reactants during the reaction, and T_c refers to the temperature of the cooling fluid. X represents the conversion of naphthalene, and d_i represents the inner diameter of the channel. C_0 refers to the initial concentration of naphthalene in the substrate, which can be calculated by eq 4. And U is the overall heat transfer coefficient defined by eq 5.

$$C_0 = \frac{n_A}{Q_{\text{Organic}} + Q_{\text{Mixed acid}}} \quad (4)$$

where n_A refers to the molar flow rate of naphthalene, Q_{Organic} and $Q_{\text{Mixed acid}}$ refer to the volume flow rate of the organic and aqueous phases, respectively. In this study, $C_0 = 1.4925 \text{ mol}\cdot\text{L}^{-1}$.

$$U = \frac{1}{\frac{1}{h} + \frac{bd_i}{\lambda d_m}} \quad (5)$$

where h represents the convective heat transfer coefficient in the microreactor, b represents the wall thickness, and λ represents the thermal conductivity coefficient of the channel wall. The channel is made of PTFE in this work, and its thermal conductivity is $0.26 \text{ W}\cdot\text{m}^{-1}\cdot\text{K}^{-1}$. And d_m represents the average of the pipe's inner and outer diameters. To simplify the calculation, the outer wall temperature was regarded as constant. In this case, $\text{Nu} = 3.66$, the convective heat transfer coefficient h can be calculated by eq 6.

$$\text{Nu} = \frac{hd_i}{\lambda_f} = 3.66 \quad (6)$$

where λ_f represents the thermal conductivity coefficient of the reactant fluid. Here, the mean thermal conductivity of the mixed fluid was used as the thermal conductivity, which is $0.275 \text{ W}\cdot\text{m}^{-1}\cdot\text{K}^{-1}$. Then, overall heat transfer coefficient U can be calculated.

The reaction rate can be expressed by eq 7:

$$\frac{dX}{dZ} = \frac{k_{app} C_0 (1 - X)(M - X)}{Q/S_r} \quad (7)$$

where k_{app} represents the apparent reaction rate constant. Since the reaction rate constants of nitration of naphthalene to 1-nitronaphthalene were rarely studied, the apparent reaction rate constant of nitration of naphthalene under the optimal process conditions was researched according to the kinetic formula in which $T_r = 30^\circ\text{C}$, $M = 1.2$, $\varphi = 74\%$.

In this experiment, the amount of 1,2-dichloroethane changed, and 0.1 mol of naphthalene was dissolved into 0.5 mol of 1,2-dichloroethane. By increasing the amount of solvent, on one hand, the occurrence of hot spots during the reaction process could be reduced, and on the other hand, the feasibility of the reaction rate constant could be verified by the previous experimental results. In addition, inline quenching replaced conventional ice–water quenching to ensure that the reaction was stopped in time. In the case of nitration, the reaction is often heterogeneous. Aromatic compounds diffuse through the organic phase into the aqueous phase and nitrate with NO^{2+} . Although nitric acid and sulfuric acid may be diffused into the organic phase in opposite directions through water, the solubility is negligible because it is quite small,³⁰ while the decoupling of mass transfer and reaction speed is very tough. Because of the relatively good mass transfer effect of microreactors, heterogeneous nitration can be regarded as a pseudohomogeneous reaction occurring in the aqueous phase, and the reaction order follows the second-order reaction widely accepted in the nitration of aromatic compounds.^{31,32}

The reaction rate of nitration can be denoted by eq 8:

$$r = k_{app} C_{\text{Nap}} C_{\text{HNO}_3}^t = k_{app} C_0^2 (1 - X)(M - X) \quad (8)$$

k_{app} denotes the apparent kinetic constant. C_{Nap} and $C_{\text{HNO}_3}^t$ represent the concentration of naphthalene and nitric acid during the reaction, respectively. By integrating eq 7 and eq 8, parameter G can be obtained by eq 9:

$$G = \frac{1}{C_0(M - 1)} \ln \left[\frac{M - X}{M(1 - X)} \right] = k_{app} t \quad (9)$$

The apparent reaction rate constant depends on only the reaction temperature. At a constant reaction temperature, the coefficient G should be linear to t with a slope k_{app} . To avoid dinitration and possible back mixing caused by a long residence time as much as possible, the residence time was set as short as possible at 5.5, 7, 9, and 11 s. The scatter plot was drawn by obtaining the reaction conversion at different reaction times, and the linear function of the Origin software was used for fitting.

The changes of reaction conversion and corresponding parameter G over time are shown in Figure 7. The small hot spot that may occur in the reaction always appeared in the first few seconds of the reaction. Hence, the conversion was high at 5.5 and 7 s and low at 11 s as the concentration decreased. Finally, the apparent rate constant $k_{app} = 0.03925 \pm 9.05746 \text{ E}^{-4} \text{ L}\cdot\text{mol}^{-1}\cdot\text{s}^{-1}$ at 30°C was obtained.

Mathematica software was used to solve the heat balance equation (eq 3) and the reaction rate equation (eq 7). The oil bath temperature was set at 30°C . When the molar ratio of dichloroethane to naphthalene was 4:1 according to experimental conditions, the reaction conversion and temperature profile along the reactor channel are shown in Figure 8.

It can be seen from Figure 8, there is a good agreement between the experimental conversion and the predicted data, indicating that the pseudohomogeneous hypothesis is feasible, and the apparent reaction rate constant obtained can meet the need for a quick estimate. However, when the reaction residence time was 10 s and the reaction residence time was above 80 s, the actual reaction conversion was slightly higher than predicted. This may be because k_{app} adopted a constant instead of the Arrhenius formula in the reaction kinetic equation. In the early stage of the reaction, the reaction rate

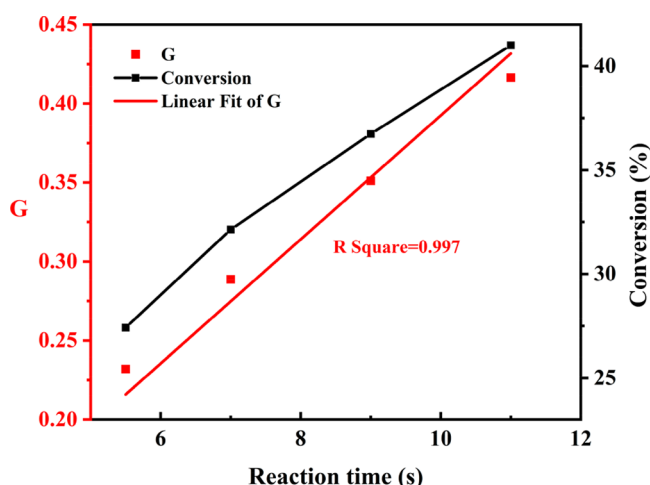


Figure 7. Determination of the apparent rate constant when sulfuric acid strength was 74%, the reaction temperature was 30 °C and the molar ratio of dichloroethane to naphthalene was 5:1.

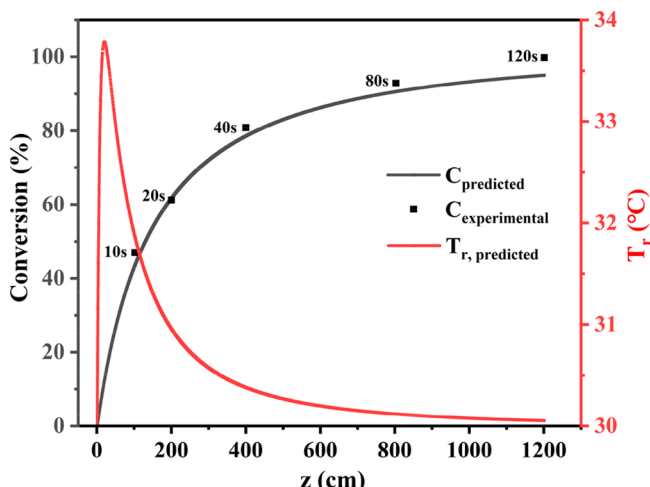


Figure 8. Change of conversion and reaction temperature profile along the reaction channel under the optimal conditions in the microreactor (when sulfuric acid strength was 74%, the reaction temperature was 30 °C, and the molar ratio of dichloroethane to naphthalene was 4:1).

increased with the increase in reaction temperature, so the reaction conversion increased. At the same time, the longer the residence time, the greater the influence caused by axial dispersion and the situation of secondary mixing, which was challenging to take into account in the quick assessment. Without considering the radial heat transfer and inlet effect, the highest temperature increase along the reaction channel was only 3.78 °C, and there was almost no overtemperature, which was consistent with the high yield and extremely low dinitration result under the optimal reaction conditions.

3.3. Scale-up of the Microreactor and Compare It with the Batch Reactor. **3.3.1. Reaction in the Mesoscale Flow Reactor.** Continuous flow reactor scale-up is mainly achieved through two aspects: numbering-up and sizing-up.³³ Based on the study in the submillimeter microreactor, the experiments were scaled up to a pilot continuous flow platform ($d_i = 4$ mm) with a temperature measuring device. Using the optimum conditions in the microchannel, the oil bath temperature was set at 30 °C, the sulfuric acid strength was set at 74%, and the molar ratio was 1.2. When the inner diameter of the reactor was enlarged from 0.8 mm to 4 mm, the mass and heat transfer performance would undoubtedly decrease.^{34,35} In this condition, the volumetric flow rate began to affect the reaction greatly. To investigate this effect, the flow rate was set at 16 mL·min⁻¹, 32 mL·min⁻¹, 48 mL·min⁻¹, and 64 mL·min⁻¹, respectively. The residence time was maintained unchanged at 2 min by using different numbers of modules. And the temperature profile under different volumetric flow rates was recorded by the real-time temperature monitoring device.

The temperature profile under different volumetric flow rates is demonstrated in Figure 9. Thermocouples 1 and 2 indicate the temperature of two preheating modules, and 3, 4, 5, and 6, respectively, indicate the outlet temperature of the reaction module 1, 2, 3, 4. Due to the limitation of the thermostat, it is difficult to maintain at 30 °C for the oil during the whole process. Hence, the temperature of the oil bath fluctuated slightly during the experiment. Especially the third and fourth reaction modules are relatively far from the oil bath machine, and their temperature fluctuations were relatively larger than the front as shown in Figure 9b.

As demonstrated in Figure 9a, for the nitration of naphthalene, the highest temperature always appeared in the first reaction module. And with the increase in volumetric flow rate, the highest temperature measured was 36.17 °C, 37.98

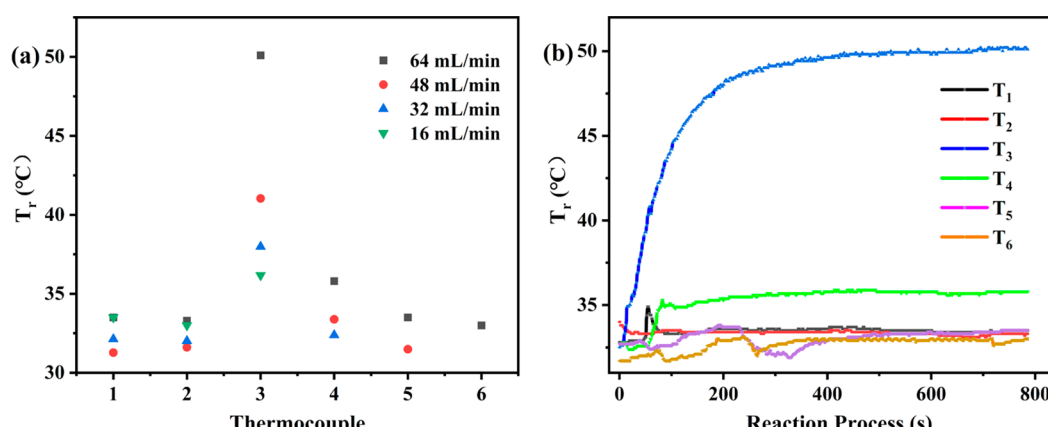


Figure 9. (a) Effect of volumetric flow rates on temperature and (b) Temperature stabilization process at a volume flow rate of 64 mL·min⁻¹.

$^{\circ}\text{C}$, $41.04\text{ }^{\circ}\text{C}$, and $50.10\text{ }^{\circ}\text{C}$, respectively. Subsequently, with the decrease in reactant concentration, the reaction rate decreased. The heat transfer capability q_{trans} exceeded the reaction heat release q_r , and the reaction temperature dropped rapidly. As the volumetric flow rate increased, the outlet temperature of the first reaction module decreased for two reasons. First of all, because the volumetric flow rate increased, the highest point of reaction temperature moved backward, the temperature measurement point of the first reaction module would be closer to the highest temperature point, and the cooling time of the reaction liquid was less so that the temperature was higher at a high volumetric flow rate when passing the first temperature measurement point. Second, because of the increase in flow rate, the mass transfer capacity increased, the reaction time limited by mass transfer decreased, and the rapid reaction in the first reaction module released more heat per unit of time, causing a higher reaction temperature.

Then the temperature profile of the experiment carried out in the pilot platform was quickly estimated by coupling the heat balance equation with the kinetic equation, as shown in Figure 10. In this condition, $Q = 64 \text{ mL}\cdot\text{min}^{-1}$.

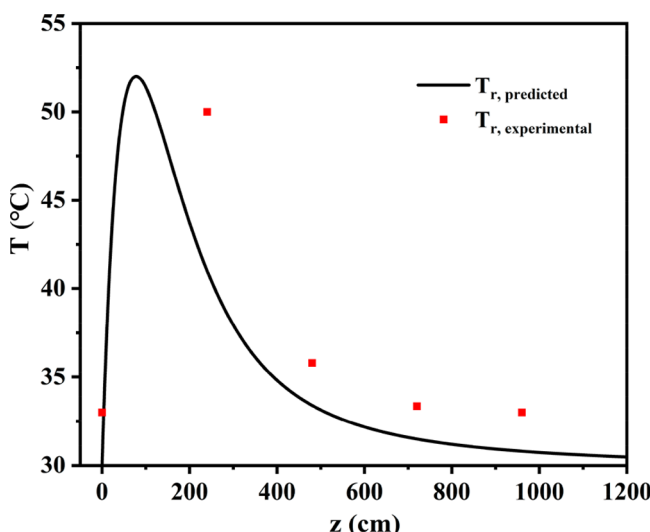


Figure 10. Quick estimated temperature profile along the pipeline when $Q = 64 \text{ mL}\cdot\text{min}^{-1}$ in the mesoscale flow reactor.

As depicted in Figure 10, the predicted highest temperature rise by the quick estimate during the reaction was $22.13\text{ }^{\circ}\text{C}$. It occurred at the point where the reaction fluid flowed to 120 cm , that is, the middle part of the first reaction module. However, when the reactants mixture flowed through the first thermocouple, its predicted temperature rise was only $11.02\text{ }^{\circ}\text{C}$, significantly different from the temperature rise of $17.10\text{ }^{\circ}\text{C}$ in the experiment. Then from the highest temperature, the reaction temperature decreased in the same trend in both experiment and prediction, first rapidly and then slowly.

The following reasons may cause this phenomenon. The primary reason is that with the increase in inner diameter, the heat transfer efficiency per unit volume of the flow reactor inevitably declined. The reaction process was fast and highly exothermic, and the heat dissipation capacity per unit volume was significantly reduced with the increase in inner diameter; therefore, the outer wall temperature could not be consistent with the coolant temperature. Instead, the outer wall temperature would rise to a higher temperature and the reaction would be further accelerated. At the same time, the temperature difference between the reactant fluid and the channel wall would decrease so that in the stage of rapid heat release the reaction temperature drop rate would slow down. In the case $\text{Nu} = 3.66$, this method is no longer applicable, resulting in a higher temperature than the predicted value at the first temperature measurement point. Second, because the preheating temperature of the pilot platform cannot be kept at $30\text{ }^{\circ}\text{C}$, the actual reaction temperature was $33\text{ }^{\circ}\text{C}$, the reaction rate was faster, and the actual reaction temperature rise should be higher. Finally, the temperature rose rapidly in the early stage of the reaction. Based on the Arrhenius formula, the reaction rate rose further and the reaction temperature should be higher than the predicted value. It can be expected that the maximum temperature increase during the actual reaction will be much higher than the $17.10\text{ }^{\circ}\text{C}$ measured by the experiment.

The analysis of the products is shown in Figure 11. As depicted in Figure 11a, the reaction conversion showed a significant upward trend from 88.83% to 100% with the increase in the volumetric flow rate. This is because when the production capacity increases with the expansion of the reactor's inner diameter, the mass transfer capacity of the reactor decreases, and the reaction is more likely to be controlled by mass transfer.³⁶ As the volumetric flow rate increased, the kinetic energy carried by the two phases increased, the flow collision became more intense, and the

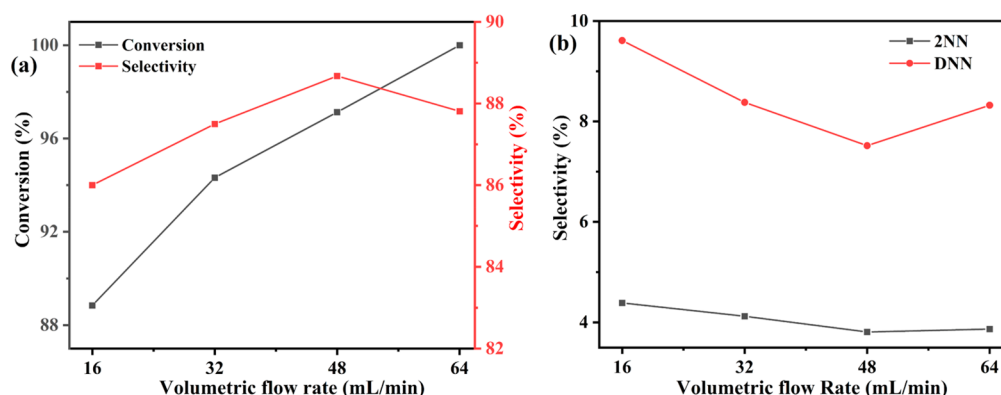


Figure 11. Influence of volumetric flow rates on reaction (a) conversion and selectivity of main product and (b) selectivity of byproduct.

mass transfer capacity was enhanced.³⁷ Therefore, the reaction conversion increased. At the same time, the selectivity of 1-nitronaphthalene was also affected by the volumetric flow rate. As the volumetric flow rate increased, the selectivity of 1-nitronaphthalene increased first and then decreased. In general, a higher temperature will increase the possibility of dinitration and decrease the selectivity of the main product. Additionally, dinitration is more likely to occur when the mass transfer capacity is poor. When naphthalene fails to diffuse from the organic phase to the water phase in time, 1-nitronaphthalene preferentially reacts with NO^{2+} to produce dinitronaphthalene. The increase in the volumetric flow rate increased the mass transfer coefficient of the system, thus enhancing the selectivity of the reaction. However, when the volume flow rate reached $64 \text{ mL}\cdot\text{min}^{-1}$, the naphthalene had wholly transformed before the end of the residence time, and only the dinitration could occur before the reaction quenching, so the selectivity showed a downward trend at the end.

As demonstrated in Figure 11b, when the reaction was scaled up to the pilot scale flow reactor, the proportion of dinitronaphthalene increased several times compared with the microreactor under the same conditions. According to the study in the microreactor, when the sulfuric acid intensity was 74% and the reaction temperature was below 40°C most of the time, the yield of dinitronaphthalene should be much lower than 8%, but the experimental result in the mesoscale flow reactor was relatively high. This is consistent with the results of the quick estimate of the temperature profile; the highest temperature rise of the reaction should appear in the first reaction module, and its highest temperature should be far more than 50.10°C so that the reaction rate in the early stage was faster. And the mass transfer was more limited in the mesoscale flow reactor, so more dinitration occurred.

3.3.2. Reaction in the Batch Reactor. For the nitration of naphthalene, the conventional production method is the semibatch reaction. In this article, the batch calorimeter RC1e was employed to study the heat release characteristics of the reaction. Based on the above research, the jacket temperature T_j was set at 30°C , the sulfuric acid strength was 74%, and the molar ratio was 1.2.

According to the research by Liang et al.,³⁸ in the batch reactor Easymax 102 Micro Reaction Calorimeter, the dosing time was usually in the range of 30–60 min, followed by an hour of holding to ensure the completion of the reaction. In this work, the dosing time and holding time were both set to 40 min. The stirring rate of the whole reaction was controlled at 300 rpm.

The whole reaction process in the batch calorimeter is depicted in Figure 12. With the addition of mixed acid, the color of the reaction liquid gradually deepened and stratification began. At the early dosing stage, mixed acid drops dispersed in the organic phase. When dosing for 40 min, a large amount of organic phase was diffused into the water phase for reaction. In the holding stage, the diffusion phenomenon was more prominent. After the end of the reaction, let it stand for 10 min, and the organic phase returned to the upper layer. It can also be seen from the apparent stratification of the reaction that the traditional batch reactor is challenging to meet the mass transfer requirements of heterogeneous fast reactions, such as nitration.

Figure 13 demonstrates the temperature profile during the reaction process. The reaction proceeded rapidly with the dosing of mixed acid, releasing a significant amount of heat. So

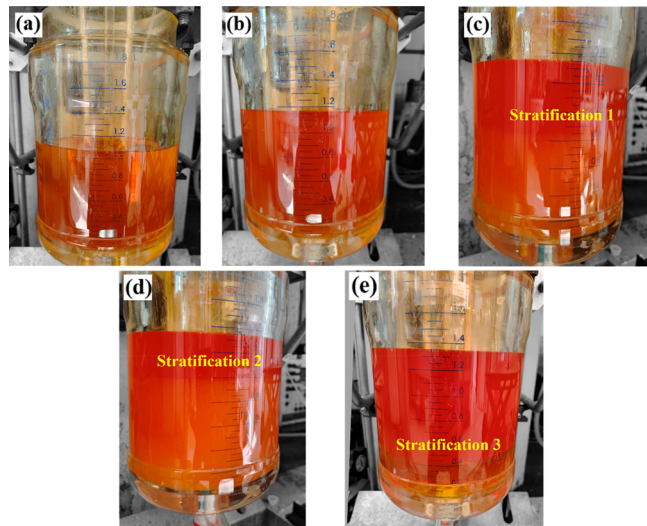


Figure 12. Reaction process in the batch reactor: (a) Dosing 10 min; (b) Dosing 20 min; (c) Dosing 40 min; (d) Holding 10 min; (e) Standing 10 min.

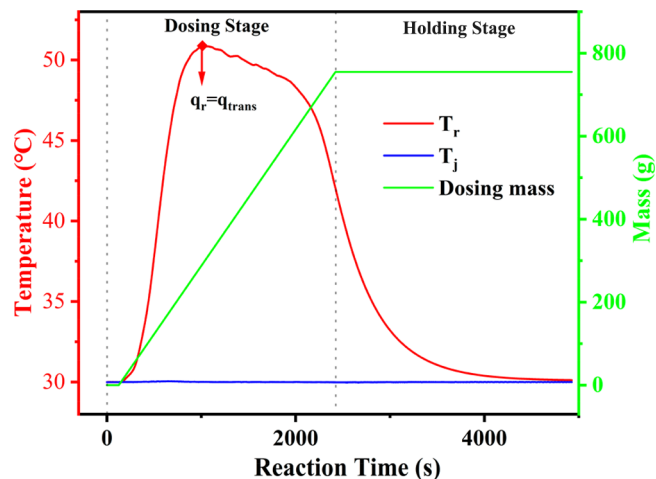


Figure 13. Temperature variation during the reaction process in the batch calorimeter.

the reaction temperature rose rapidly in the early dosing stage, which brought about the rise of the reaction rate, and the heat release rate increased accordingly. T_r reached its highest value of 50.93°C when the mixed acid was added for 1012 s. At this time, with the decrease in the reactant concentration and the increase in the temperature difference between the reactant and the jacket temperature, the reaction heat release rate q_r was equal to the heat transfer rate q_{trans} . Subsequently, the decrease of organic phase concentration played a leading role in the reaction rate, and the generation of water brought about a NO^{2+} decrease in concentration so that the heat transfer rate could meet the demand for heat transfer, and the reaction temperature began to decrease. After the end of dosing, the temperature decline trend increased again compared with the previous, and the reactant cooled, rapidly decreasing to around 30°C . In the whole reaction process, the time when the temperature of the reaction system exceeded the setting temperature by 15°C was 2240 s, accounting for 93.3% of the entire dosing time, and the time when the temperature exceeded the setting temperature by 10°C reached 2540 s, accounting for 52.91% of the total reaction time. The

maximum temperature rise during the reaction was 20.93 °C. It can be seen from the above study that the reaction temperature played a vital role in the selectivity and yield of the reaction. Long-term overtemperature in the batch reactor would increase the reaction risk and reduce the output.

Figure 14 shows the conversion and selectivity of the nitration in the semibatch reaction. The reaction conversion

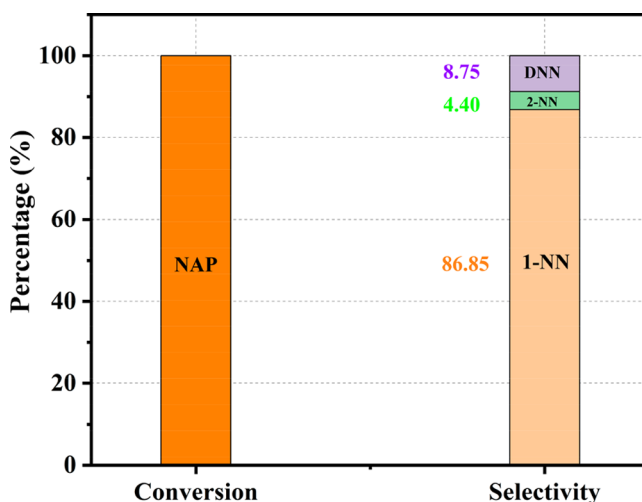


Figure 14. Reaction conversion and selectivity in the batch reactor.

reached 100%, the selectivity of 1-nitronaphthalene reached 86.85%, and the products of 2-nitronaphthalene and dinitration accounted for 4.30% and 8.86% of the total products, respectively. For a traditional laboratory-scale batch reactor, the total volumetric mass transfer coefficient of a liquid–liquid heterogeneous system ranges from 0.001 to 0.02 s⁻¹.³⁹ However, in the microreactor, the surface area is large, the contact area between the two phases is significantly increased, and the interface refresh frequency is high, which makes the overall mass transfer coefficient of the microreactor 2–3 orders of magnitude larger than that of the traditional tank reactor, usually in the range of 0.05–15 s⁻¹.⁴⁰ At the low mass transfer coefficient, the relatively high yield was due to the low sulfuric acid strength and the reaction setting temperature, so the dinitration occurred less. However, compared with the performance in the microreactor under the same conditions, the selectivity of 2-nitronaphthalene was close to that of continuous flow mode at 50 °C, and the selectivity of dinitration products was much greater than that of continuous flow mode. This is because the whole dosing process of the semibatch reaction was almost all in the state of overtemperature 15 °C. And for the batch reactor, the mass transfer capacity was challenging to meet the mass transfer demand when the reaction rate was relatively fast, the reaction may be subject to mass transfer control for a longer time, and more 1-nitronaphthalene reacted with nitric acid to produce dinitronaphthalene.

3.3.3. Comparison of Flow and Batch Reactor. Table 1 shows a comparison between the batch reactor and the mesoscale flow reactor.

For the semibatch reaction, to make sure that the reaction was complete, the whole reaction process was up to 80 min. Even if the holding time was removed, the dosing time reached 40 min. While in continuous flow reaction, the same conversion and a higher selectivity could be achieved within

Table 1. Comparison between Semibatch Mode and Continuous Flow Mode

	Semibatch mode	Continuous mode ^a
Reaction time (s)	4800	120
Highest overtemperature (°C)	50.9	>50.1
Time duration of over temperature (s) ^b	2340	30–60
Pressure (Mpa)	0	0.135 MPa
Total inventory in the reactor (mL)	1340	128
Yield (%)	86.85	87.81
Space-Time-Yield (g·L ⁻¹ ·s ⁻¹)	0.0361	1.575
Annual production (kg·a ⁻¹) ^c	684.3	2643

^aData from $Q = 60 \text{ mL} \cdot \text{min}^{-1}$. ^bExceeding the setting temperature by more than 10 °C was seen as overtemperature. ^c3000 h of work per year.

only 120 s, which made the space–time yield of continuous flow reaction 2 orders of magnitude higher than that of semibatch reaction. At the same working time each year, the continuous flow mode could achieve more than three times the annual output even if its inventory was smaller. However, the reaction yield in the flow mode was not much higher than that in the batch reactor, which may be attributed to the actual temperature increase of the reaction process in the pilot scale flow reactor well exceeding 17.1 °C. As a result, the same dinitration occurred at a shorter overtemperature time.

Regarding inherent safety, although the maximum temperature during the reaction measured by the two reactors was similar, the continuous flow reactor could quickly reduce the reaction temperature to below 40 °C. Compared with the ultralong overtemperature time of the 2340 s in the batch reactor, the overtemperature time of continuous flow mode was between 30 to 60 s.

For the traditional batch reaction, the temperature and conversion of the reaction process are often related to the reaction time and there is always a corresponding conversion and reaction temperature at a specific time. Therefore, the reaction rate can only be seen as a function of time $r = f(t)$ for the batch reaction. However, for the continuous flow reaction, the temperature profile and conversion during the reaction process change along the channel with the evolution of reaction conditions, so the reaction rate of the continuous flow mode can be regarded as spatially related, that is, $r = f(z)$. Changing the reaction rate relative to time to space makes it much easier to deal with the problem of overtemperature and even thermal runaway that may occur during the reaction. For the rapid exothermic reaction, such as the nitration of naphthalene, the channel material of the reaction module with the fastest reaction rate can be replaced with channels with higher thermal conductivity to ensure that the wall temperature in the reaction process can be as consistent as possible with the temperature of the coolant. The diameter of the channel at the initial stage of the reaction can be reduced to obtain a higher overall heat transfer coefficient. Even temperature control of the first reaction module can be carried out separately to achieve process safety for the entire reaction. And it will not affect the subsequent reaction in the channel, which is challenging to accomplish for the batch reactor. Therefore, compared with the batch reactor, the continuous flow reactor is more inherently safe and efficient.

4. CONCLUSION

In this work, the effects of the residence time, reaction temperature, sulfuric acid strength, and molar ratio on the nitration reaction were systematically investigated. When the residence time was 120 s, the reaction temperature was 30 °C, and the sulfuric acid strength was 74%, the highest yield could reach 94.96%. By coupling the energy conservation equation and mass conservation equation, the temperature profile of the reaction fluid along the channel was quickly estimated. The results show that the maximum temperature increase during the reaction process was only 3.78 °C, and there was no overtemperature effect.

Then the reaction process was scaled up to a mesoscale flow reactor platform to meet the needs of industrial production. And a comparison of the mesoscale flow reactor and conventional semibatch reactor was conducted. Although the highest temperatures during the reaction of both reactors all reached more than 50 °C, the higher overall heat transfer coefficient of the continuous flow mode could quickly control the reaction temperature below the overtemperature range. While, in the semibatch reaction, the temperature rise of almost the whole dosing stage was above 15 °C. In addition, for the mesoscale flow reactor, the space–time yield could reach 1.575 g·L⁻¹·s⁻¹, which was 2 orders of magnitude higher than that of the batch reactor. When the annual working time was set to 3000 h, the annual output of the mesoscale flow reactor could reach 2643 kg·a⁻¹.

The continuous flow mode transfers the reaction from the traditional time-related to the space-related, which makes the whole reaction easier to control, more stable, and more in line with the inherent safety requirements. Therefore, we envisage that compared with conventional batch mode, continuous flow mode is more suitable for fast and highly exothermic reactions.

■ ASSOCIATED CONTENT

SI Supporting Information

The Supporting Information is available free of charge at <https://pubs.acs.org/doi/10.1021/acs.oprd.3c00282>.

Detailed experiment information in the microreactor, including the reaction product analysis from 10 to 120 s under all selected reaction temperatures and sulfuric acid strengths, is shown in the Supporting Information. ([PDF](#))

■ AUTHOR INFORMATION

Corresponding Authors

Juncheng Jiang – College of Safety Science and Engineering, Nanjing Tech University, Nanjing 211816, China; [ORCID.org/0000-0001-7018-2709](#); Email: junchengjiang@njtech.edu.cn

Zhiqian Chen – College of Safety Science and Engineering, Nanjing Tech University, Nanjing 211816, China; Email: chenzq@njtech.edu.cn

Authors

Feng Xu – College of Safety Science and Engineering, Nanjing Tech University, Nanjing 211816, China

Lei Ni – College of Safety Science and Engineering, Nanjing Tech University, Nanjing 211816, China; [ORCID.org/0000-0001-5941-6156](#)

Gang Fu – College of Safety Science and Engineering, Nanjing Tech University, Nanjing 211816, China; [ORCID.org/0000-0001-8060-4215](#)

Jian Liu – College of Safety Science and Engineering, Nanjing Tech University, Nanjing 211816, China

Complete contact information is available at: <https://pubs.acs.org/10.1021/acs.oprd.3c00282>

Notes

The authors declare no competing financial interest.

■ ACKNOWLEDGMENTS

The authors are grateful to the National Natural Science Foundation of China (grant numbers 52274209), the Jiangsu Province Excellent Postdoctoral Program (2023ZB484), and the Postgraduate Research & Practice Innovation Program of Jiangsu Province (SJCX23_0461) for their financial support of this study.

■ NOMENCLATURE

b	wall thickness, m
C_0	initial concentration of naphthalene in the substrate, mol·m ⁻³
$C_{\text{HNO}_3}^t$	concentration of nitric acid, mol·m ⁻³
C_{Nap}	concentration of naphthalene, mol·m ⁻³
c_p	average specific heat capacity, J·g ⁻¹ ·K ⁻¹
d_i	inner diameter of the channel, m
d_m	the average of the channel's inner and outer diameters, m
d_o	outer diameter of the channel, m
h	convective heat transfer coefficient, W·m ⁻² ·K ⁻¹
k_{app}	apparent kinetic constant, L·mol ⁻¹ ·s ⁻¹
M	the molar ratio of nitric acid to naphthalene
M_{Nap}	the molar mass of naphthalene, g·mol ⁻¹
$M_{1-\text{Nap}}$	the molar mass of 1-nitronaphthalene, g·mol ⁻¹
m_{or}	mass of the organic phase, g
$m_{\text{Nap},0}$	feeding mass of naphthalene, g
n_A	molar flow rate of naphthalene, mol·L ⁻¹
Nu	Nusselt number
Q	average volumetric flow rate, mL·min ⁻¹
q_r	heat release rate, W
q_{trans}	heat transfer rate, W
S	selectivity of products, %
S_r	cross-sectional area of the channel, m ²
T_c	temperature of the cooling fluid, °C
T_j	temperature of oil in the jacket, °C
T_r	temperature of reactants, °C
U	Overall heat transfer coefficient, W·m ⁻² ·K ⁻¹
w_{Nap}	mass fraction of naphthalene in the organic phase, %
$w_{1-\text{Nap}}$	mass fraction of 1-nitronaphthalene, %
X	conversion of naphthalene, %
Z	channel length, m
λ	thermal conductivity of the channel, W·m ⁻¹ ·K ⁻¹
λ_f	thermal conductivity of the reactant fluid, W·m ⁻¹ ·K ⁻¹
φ	sulfuric acid strength, %

■ REFERENCES

- (1) Brocklehurst, C. E.; Lehmann, H.; La Vecchia, L. Nitration Chemistry in Continuous Flow Using Fuming Nitric Acid in a Commercially Available Flow Reactor. *Org. Process Res. Dev.* **2011**, *15* (6), 1447–1453.

- (2) Russo, D.; Onotri, L.; Marotta, R.; Andreozzi, R.; Di Somma, I. Benzaldehyde Nitration by Mixed Acid under Homogeneous Condition: A Kinetic Modeling. *Chem. Eng. J.* **2017**, *307*, 1076–1083.
- (3) Kulkarni, A. A. Continuous Flow Nitration in Miniaturized Devices. *Beilstein J. Org. Chem.* **2014**, *10*, 405–424.
- (4) Saada, R.; Patel, D.; Saha, B. Causes and Consequences of Thermal Runaway Incidents—Will They Ever Be Avoided? *Process Saf. Environ. Prot.* **2015**, *97*, 109–115.
- (5) Zhang, L. S.; Ruan, J.; Lu, Z. Y.; Xu, Z. S.; Lan, G. C.; Wang, J. L. Thermal Hazard Assessment of 3-Nitro-1,2,4-Triazole-5-One (NTO) Synthesis. *Process Saf. Environ. Prot.* **2022**, *166*, 649–655.
- (6) Capaldo, L.; Wen, Z.; Noel, T. A Field Guide to Flow Chemistry for Synthetic Organic Chemists. *Chem. Eng. Sci.* **2023**, *14* (16), 4230–4247.
- (7) Guo, S.; Zhan, L.; Zhu, G.; Wu, X.; Li, B. Scale-Up and Development of Synthesis 2-Ethylhexyl Nitrate in Microreactor Using the Box–Behnken Design. *Org. Process Res. Dev.* **2022**, *26* (1), 174–182.
- (8) Li, G. X.; Shang, M. J.; Song, Y.; Su, Y. H. Characterization of Liquid–Liquid Mass Transfer Performance in a Capillary Microreactor System. *AIChE J.* **2018**, *64* (3), 1106–1116.
- (9) Wang; Ni, L.; Wang, J.; Xu, F.; Jiang, J.; Chen, Z.; Fu, G.; Pan, Y. Experimental and Numerical Study of the Synthesis of Isopropyl Propionate in Microreactor. *Chem. Eng. Process.* **2022**, *170*, 108705.
- (10) Wang, K.; Zhang, J. S.; Zheng, C.; Dong, C.; Lu, Y. C.; Luo, G. S. A Consecutive Microreactor System for the Synthesis of Caprolactam with High Selectivity. *AIChE J.* **2015**, *61* (6), 1959–1967.
- (11) Hafner, M.; Wolff, F.; Roeder, T. Continuous Diameter Increase Reactor – a Reactor Concept for Maximizing Productivity by a Controlled Diameter Extension. *J. Flow Chem.* **2022**, *12* (3), 247–254.
- (12) LaPorte, T. L.; Wang, C. Continuous Processes for the Production of Pharmaceutical Intermediates and Active Pharmaceutical Ingredients. *Curr. Opin. Drug. Disc.* **2007**, *10* (6), 738–745.
- (13) Calabrese, G. S.; Pissavini, S. From Batch to Continuous Flow Processing in Chemicals Manufacturing. *AIChE J.* **2011**, *57* (4), 828–834.
- (14) Burns, J. R.; Ramshaw, C. A Microreactor for the Nitration of Benzene and Toluene. *Chem. Eng. Commun.* **2002**, *189* (12), 1611–1628.
- (15) Su, Y. H.; Zhao, Y. C.; Jiao, F. J.; Chen, G. W.; Yuan, Q. The Intensification of Rapid Reactions for Multiphase Systems in a Microchannel Reactor by Packing Microparticles. *AIChE J.* **2011**, *57* (6), 1409–1418.
- (16) Yu, Z. Q.; Zhou, P. C.; Liu, J. M.; Wang, W. Z.; Yu, C. M.; Su, W. K. Continuous-Flow Process for Selective Mononitration of 1-Methyl-4-(Methylsulfonyl)Benzene. *Org. Process Res. Dev.* **2016**, *20* (2), 199–203.
- (17) Wen, Z. H.; Jiao, F. J.; Yang, M.; Zhao, S. N.; Zhou, F.; Chen, G. W. Process Development and Scale-up of the Continuous Flow Nitration of Trifluoromethoxybenzene. *Org. Process Res. Dev.* **2017**, *21* (11), 1843–1850.
- (18) Li, L.; Yao, C. Q.; Jiao, F. J.; Han, M.; Chen, G. W. Experimental and Kinetic Study of the Nitration of 2-Ethylhexanol in Capillary Microreactors. *Chem. Eng. Process.* **2017**, *117*, 179–185.
- (19) Chen, P.; Shen, C.; Qiu, M.; Wu, J.; Bai, Y.; Su, Y. Synthesis of S-Fluoro-2-Nitrobenzotrifluoride in a Continuous-Flow Millireactor with a Safe and Efficient Protocol. *J. Flow Chem.* **2020**, *10* (1), 207–218.
- (20) Zhao, H. L.; Liu, S. E.; Shang, M. J.; Su, Y. H. Direct Oxidation of Benzene to Phenol in a Microreactor: Process Parameters and Reaction Kinetics Study. *Chem. Eng. Sci.* **2021**, *246*, 116907.
- (21) Hussain, A.; Sharma, M.; Patil, S.; Acharya, R. B.; Kute, M.; Waghchaure, A.; Kulkarni, A. A. Design and Scale-up of Continuous Di-Nitration Reaction Using Pinched Tube Flow Reactor. *J. Flow Chem.* **2021**, *11* (3), 611–624.
- (22) Cui, Y.; Song, J.; Du, C.; Deng, J.; Luo, G. Determination of the Kinetics of Chlorobenzene Nitration Using a Homogeneously Continuous Microflow. *AIChE J.* **2022**, *68* (4). DOI: [10.1002/aic.17564](https://doi.org/10.1002/aic.17564).
- (23) Chen, Y. Z.; Zhao, Y. C.; Han, M.; Ye, C. B.; Dang, M. H.; Chen, G. W. Safe, Efficient and Selective Synthesis of Dinitro Herbicides via a Multifunctional Continuous-Flow Microreactor: One-Step Dinitration with Nitric Acid as Agent. *Green Chem.* **2013**, *15* (1), 91–94.
- (24) Gong, S. W.; Liu, L. J.; Zhang, J. L.; Cui, Q. X. Stable and Eco-Friendly Solid Acids as Alternative to Sulfuric Acid in the Liquid Phase Nitration of Toluene. *Process Saf. Environ. Prot.* **2014**, *92* (6), 577–582.
- (25) Li, S. F.; Zhang, X. L.; Ji, D. S.; Wang, Q. Q.; Jin, N.; Zhao, Y. C. Continuous Flow Nitration of 3-[2-Chloro-4-(Trifluoromethyl) Phenoxy] Benzoic Acid and Its Chemical Kinetics within Droplet-Based Microreactors. *Chem. Eng. Sci.* **2022**, *255*, 117657.
- (26) Rahaman, M.; Mandal, B.; Ghosh, P. Nitration of Nitrobenzene at High-Concentrations of Sulfuric Acid: Mass Transfer and Kinetic Aspects. *AIChE J.* **2010**, *56* (3), 737–748.
- (27) Sharma, Y.; Joshi, R. A.; Kulkarni, A. A. Continuous-Flow Nitration of o-Xylene: Effect of Nitrating Agent and Feasibility of Tubular Reactors for Scale-Up. *Org. Process Res. Dev.* **2015**, *19* (9), 1138–1147.
- (28) Fath, V.; Szmais, S.; Lau, P.; Kockmann, N.; Roder, T. Model-Based Scale-Up Predictions: From Micro-to Millireactors Using Inline Fourier Transform Infrared Spectroscopy. *Org. Process Res. Dev.* **2019**, *23* (9), 2020–2030.
- (29) Westermann, T.; Mleczko, L. Heat Management in Microreactors for Fast Exothermic Organic Syntheses—First Design Principles. *Org. Process Res. Dev.* **2016**, *20* (2), 487–494.
- (30) Olah, G. A.; Malhotra, R.; Narang, S. C. NITRATION: Methods and Mechanisms. In *World Scientific Series in 20th Century Chemistry*; World Scientific Publishing Company: 2003; Vol. 11, pp 975–979. DOI: [10.1142/9789812791405_0192](https://doi.org/10.1142/9789812791405_0192).
- (31) Mandal, A. K.; Kunjir, G. M.; Singh, J.; Adhav, S. S.; Singh, S. K.; Pandey, R. K.; Bhattacharya, B.; Lakshmi Kantam, M. Optimization of Ammonium Sulfamate Nitration for the Preparation of Ammonium Dinitramide. *Cent. Eur. J. Energy Mater.* **2014**, *11* (1), 83–97.
- (32) Song, J.; Cui, Y. J.; Sheng, L.; Wang, Y. J.; Du, C. C.; Deng, J.; Luo, G. S. Determination of Nitration Kinetics of P-Nitrotoluene with a Homogeneously Continuous Microflow. *Chem. Eng. Sci.* **2022**, *247*, 117041.
- (33) Kockmann, N.; Gottsponer, M.; Roberge, D. M. Scale-up Concept of Single-Channel Microreactors from Process Development to Industrial Production. *Chem. Eng. J.* **2011**, *167* (2–3), 718–726.
- (34) Kockmann, N.; Roberge, D. M. Scale-up Concept for Modular Microstructured Reactors Based on Mixing, Heat Transfer, and Reactor Safety. *Chem. Eng. Process.* **2011**, *50* (10), 1017–1026.
- (35) Sagandira, C. R.; Watts, P. A Study on the Scale-up of Acyl Azide Synthesis in Various Continuous Flow Reactors in Homogeneous and Biphasic Systems. *J. Flow Chem.* **2018**, *8* (2), 69–79.
- (36) Biswas, K. G.; Das, G.; Ray, S.; Basu, J. K. Mass Transfer Characteristics of Liquid–Liquid Flow in Small Diameter Conduits. *Chem. Eng. Sci.* **2015**, *122*, 652–661.
- (37) Wang, X. D.; Wang, Y. M.; Li, F.; Li, L.; Ge, X. H.; Zhang, S. L.; Qiu, T. Scale-up of Microreactor: Effects of Hydrodynamic Diameter on Liquid–Liquid Flow and Mass Transfer. *Chem. Eng. Sci.* **2020**, *226*, 115838.
- (38) Liang, J.; Ni, L.; Wu, P.; Yao, H.; Chen, Q.; Fu, G.; Jiang, J. Process Safety Assessment of Semibatch Nitration of Naphthalene with Mixed Acid to 1-nitronaphthalene. *AIChE J.* **2022**, *68* (7). DOI: [10.1002/aic.17679](https://doi.org/10.1002/aic.17679).
- (39) Hartman, R. L.; McMullen, J. P.; Jensen, K. F. Deciding Whether To Go with the Flow: Evaluating the Merits of Flow Reactors for Synthesis. *Angew. Chem., Int. Ed.* **2011**, *50* (33), 7502–7519.
- (40) Fu, G.; Ni, L.; Wei, D.; Jiang, J. C.; Chen, Z. Q.; Pan, Y. Scale-up and Safety of Toluene Nitration in a Meso-Scale Flow Reactor. *Process Saf. Environ. Prot.* **2022**, *160*, 385–396.